Jurnal Teknologi

Full Paper

CFD MODELING OF SO_2 CAPTURE USING LIMESTONE IN INDUSTRIAL SCALE CIRCULATING FLUIDIZED BED BOILER

Rattapong Tritippayanon[a,b], Veeraya Jiradilok[c], Pornpote Piumsomboon[a], Benjapon Chalermsinsuwan[a,b*]

[a]Department of Chemical Technology, Faculty of Science, Chulalongkorn University, 254 Phayathai Road, Patumwan, Bangkok 10330, Thailand
[b]Center of Excellence on Petrochemical and Materials Technology, Chulalongkorn University, 254, Phayathai Road, Patumwan, Bangkok 10330, Thailand
[c]D.A. Research Center Co., Ltd., 122 Moo 2, Thatoom, Srimahaphote, Prachinburi 25140, Thailand

Article history
Received
18 June 2015
Received in revised form
10 September 2015
Accepted
13 December 2015

*Corresponding author
benjapon.c@chula.ac.th

Graphical abstract

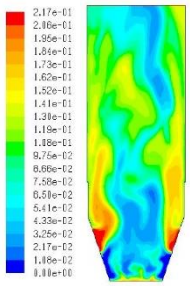

OXYGEN MOLE FRACTION CONTOUR

Abstract

The unsteady state computational fluid dynamics model for gas-solid particle flow in industrial scale circulating fluidized bed boiler combining with combustion and desulfurization (using limestone solid sorbent) chemical reactions, both homogeneous and heterogeneous, was developed in this study. The effects of solid sorbent feeding position and solid sorbent particle size on sulfur dioxide concentration were investigated. The results showed that both the solid sorbent feeding position and solid sorbent particle size had an effect on the sulfur dioxide capture. Entering solid sorbent at the upper secondary air position gave lower sulfur dioxide concentration than the one at the lower secondary air position and fuel feed position, respectively. This can be explained by the influence of suitable temperature at the upper secondary air position for desulfurization chemical reaction. About the solid sorbent particle size, the sulfur dioxide capture was the lowest when using the largest solid sorbent particle size due to the system hydrodynamics.

Keywords: CFD modeling, circulating fluidized bed boiler, combustion, desulfurization, sulfur dioxide capture

1.0 INTRODUCTION

The increasing of world population leads to a higher energy demand. Currently, the coal-biomass power plants are still the important source of energy. However, the fuel power plant operation will lead to the significant amount of pollution emissions including sulfur dioxide gas (SO_2). This SO_2 gas can cause the acid rain, climate change and human health problems [1]. The limestone ($CaCO_3$) is a well-known solid sorbent to react with the flue gas from power plants. This is because it can be easily combined with the conventional combustion power plant process and it has low price [2, 3].

For the controlling of SO_2 emission, some alternative solutions to capture SO_2 gas are explored in the literature such as altering the solid sorbent circulation rates and the solid sorbent inventory [4]. However, the effect of other process conditions is still unknown.

Circulating fluidized bed (CFB) has been extensively used in chemical, petrochemical and energy industries, especially power generation, because it gives high combustion efficiency. In CFB boiler, the solid particle and gas phases react with each other in the riser section. In addition, the CFB boiler has the

cyclone and downer sections to separate large or unreacted solid particles and to return them into the process [5-6].

Computational fluid dynamics (CFD) are recently used mathematical tool for predicting the engineering problem. This method can accurately predict the flow behavior, heat and mass transfers and chemical reactions by using numerical approaches. The advantages of using this method are being easy to use even in the non-safe process operating condition and reducing the cost and time on the real experiment [7-8].

In this study, the modeling SO_2 capture using $CaCO_3$ in industrial scale CFB boiler therefore was developed using CFD simulation. At first, the developed model was compared its correctness with the actual collecting data from a power plant, including the outlet SO_2 concentration, the outlet oxygen (O_2) concentration and the outlet system gas velocity. Then, the effects of solid sorbent feeding position and solid sorbent particle size on SO_2 concentration were investigated to propose the appropriate guidelines for SO_2 capture.

2.0 MODEL DESCRIPTION

The configuration and detailed dimension of the simplified riser section of a CFB boiler are shown in Figure 1. The employed model was two-dimensional model. The maximum dimensions of the height and diameter of CFB boiler were 20.00 m and 7.96 m, respectively. Fuel entered the system at fuel feed position at 1.23 m from the primary air position. The auxiliary air was fed to the system at two positions to improve the combustion efficiency. The lower and upper secondary airs entered the system at 2.37 and 3.80 m from the primary air position, respectively. In addition, all the three input positions were fed with 30° of depression.

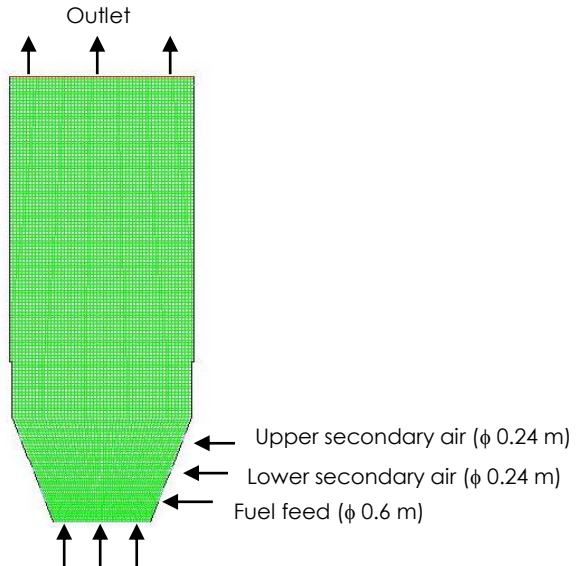

Figure 1 Dimension of the riser section of industrial scale CFB boiler

The model was unsteady state Eulerian-Eulerian CFD model. The governing, including momentum, energy and mass conservation equations, and constitutive equations were solved separately for each phase as the continuous (gas) and dispersed (solid particles) phases [9-10]. About the constitutive equations, the set of equations was selected from the kinetic theory of granular flow theory. This theory was effectively employed in many literatures on CFB boiler modelling.

2.1 Chemical Reaction Conditions

The chemical reactions of solid particle phase consisting of fuel solid particle (lower calorific value (LCV) coal, higher calorific value (HCV) coal and biomass (wood chip)) and $CaCO_3$ (sorbent) solid particle are shown below:

$$\text{Fuel} \rightarrow \text{Volatile} + \text{Char} + \text{Ash} \quad (R_1)$$

$$CH_4 + \frac{3}{2}O_2 \rightarrow CO + 2H_2O \quad (R_2)$$

$$C_2H_6 + \frac{5}{2}O_2 \rightarrow 2CO + 3H_2O \quad (R_3)$$

$$CO + \frac{1}{2}O_2 \rightarrow CO_2 \quad (R_4)$$

$$H_2 + \frac{1}{2}O_2 \rightarrow H_2O \quad (R_5)$$

$$C_{(s)} + \frac{1}{K}O_{2\,(g)} \rightarrow \left(2 - \frac{2}{K}\right)CO_{\,(g)} + \left(\frac{2}{K} - 1\right)CO_{2\,(g)} \quad (R_6)$$

$$C_{(s)} + CO_{2\,(g)} \rightarrow 2CO_{\,(g)} \quad (R_7)$$

$$CaCO_3 \rightarrow CaO + CO_2 \quad (R_8)$$

$$CaO + SO_2 + \frac{1}{2}O_2 \rightarrow CaSO_4 \quad (R_9)$$

First, the fuel solid particles were dried and devolatilized (R_1). The volatile matter includes methane (CH_4), ethane (C_2H_6), carbon monoxide (CO), CO_2, water vapour (H_2O) and hydrogen (H_2). Then, the combustion of volatile (R_2-R_5), the combustion of char (R_6), the gasification of char (R_7) and the capturing of impurity gas (R_8-R_9) reactions were occurred.

For the drying and devolatilization reaction (R_1), this step was assumed to be fast reaction step. The fraction of char, ash and volatile gas composition were then determined based on real experimental information using the proximate and ultimate analysis of each fuel solid particle [11-12] as shown in Tables 1, 2 and 3. Then, the overall gas compositions were obtained according to the feeding weight percent of each fuel component. The obtained specie mass fractions of volatile gas composition are 0.046 for CH_4, 0.057 for C_2H_6, 0.226 for CO, 0.031 for CO_2, 0.580 for H_2O, 0.030 for H_2, 0.013 for SO_2 and 0.015 for NO_2 respectively.

Table 1 Analysis of coal (HCV)'s properties

Proximate (wt%)		Ultimate (wt%)	
Fixed carbon	38.29	C	51.17
Volatile matter	29.00	H	3.91
Ash	8.54	N	1.27
Moisture	24.17	O	10.19
		S	0.76

Table 2 Analysis of coal (LCV)'s properties

Proximate (wt%)		Ultimate (wt%)	
Fixed carbon	31.68	C	45.96
Volatile matter	33.29	H	3.75
Ash	4.79	N	0.62
Moisture	30.24	O	14.16
		S	0.48

Table 3 Analysis of biomass (wood chip)'s properties

Proximate (wt%)		Ultimate (wt%)	
Fixed carbon	21.59	C	27.43
Volatile matter	33.05	H	2.55
Ash	0.36	N	0.07
Moisture	45.00	O	24.59
		S	0.01

The combustion of volatile component occurred according to various homogeneous chemical reactions. The homogeneous chemical reactions included the CH_4 oxidation (R_2), C_2H_6 oxidation (R_3), CO combustion (R_4) and H_2 oxidation (R_5). Their reaction rate and chemical reaction kinetics are summarized in Table 4 [13-15].

The solid fuel heterogeneous chemical reactions consisted of the char combustion (R_6) [16] and the boudouard reaction (R_7). Their reaction rate and chemical kinetic constants are also summarized in Table 4 [14-17].

Generally, the desulfurization process using solid sorbents consisted of indirect and direct desulfurization mechanisms. In this study, $CaCO_3$ was calcined to be CaO and CO_2 (R_7). Then, the CaO was used as the sorbent for SO_2 capture [5, 18-20]. Therefore, the $CaCO_3$ solid particles consisted of pseudo-species, including $CaCO_3$, CaO and $CaSO_4$. The calcinations reaction (R_8) took place at system temperature between 873-1,273 K. However, some literature study claimed that the proper operating temperature was between 1,073-1,173 K [5, 21, 22]. This is because the temperature in this range was appropriate for driven the chemical reaction of SO_2 capture. Their reaction rate and chemical kinetic constants are summarized in Table 4. In this study, the employed reaction rates were obtained from the similar fluidized bed literatures [5, 22].

Table 4 Reaction rates used in the simulations [5, 22].

	Reaction rate	Reaction rate constant
R_1	R_1	Experimental data
R_2	$R_2 = k_2\left(\frac{Y_{O_2}\rho_g}{M_{O_2}}\right)^{0.8}\left(\frac{Y_{CH_4}\rho_g}{M_{CH_4}}\right)^{0.7}$	$k_2 = 1.58 \times 10^{10} \exp\left(\frac{-24243}{T_g}\right)$
R_3	$R_3 = k_3\left(\frac{Y_{C_2H_6}\rho_g}{M_{C_2H_6}}\right)\left(\frac{Y_{O_2}\rho_g}{M_{O_2}}\right)$	$k_3 = 1.585 \times 10^{10} \exp\left(\frac{-24157}{T_g}\right)$
R_4	$R_4 = k_4\, Y_{CO} Y_{H2O}{}^{0.5} \frac{17.5 Y_{O_2}}{1+24 Y_{O_2}}\left(\frac{p}{RT_g}\right)^{1.8}$	$k_4 = 3 \times 10^{10} \exp\left(\frac{-8.699\times10^7}{RT_g}\right)$
R_5	$R_5 = k_5\left(\frac{Y_{O_2}\rho_g}{M_{O_2}}\right)\left(\frac{Y_{H_2}\rho_g}{M_{H_2}}\right)^{1.5}$	$k_5 = 1.63 \times 10^9\, T_g{}^{1.5} \exp\left(\frac{-3420}{T_g}\right)$
R_6	$R_6 = \frac{6\alpha_{s1}\rho_{s1}Y_c}{d_{s1}\rho_s} k_6\, Y_{O_2}$	$k_6 = \frac{RT_{s1}/M_c}{(1/k_{cr})+(1/k_{cd})}$, $k_{cr} = 8910\, exp\left(\frac{-1.4947\times10^8}{RT_{s1}}\right)$, $k_{cd} = \frac{Shp\left(D_g+\frac{\mu_g}{\rho_g Sc_i}\right)M_c}{d_{s1}R_gT_g}$
R_7	$R_7 = \frac{k_7 Y_{CO_2} Y_c}{1+k_{7,CO_2}Y_{CO_2}+k_{7,CO}Y_{CO}}$	$k_7 = 3.1785\text{x}10^{10}\exp\left(\frac{-2.65\times10^8}{RT_{s1}}\right)$, $k_{7,CO_2} = 66\exp\left(\frac{-2.55\times10^7}{RT_{s1}}\right)$, $k_{7,CO} = 120\exp\left(\frac{-2.55\times10^7}{RT_{s1}}\right)$
R_8	$R_8 = k_8\alpha_{s2}\rho_{s2}Y_{CaCO_3}S_{CaCO_3}\frac{p_e-p_{CO_2}}{p_e}$	$k_8 = 6.078\text{x}10^4\exp\left(\frac{-2.05\times10^8}{RT_{s1}}\right)$, $p_e = 4.192\text{x}10^{12}\exp\left(\frac{-1.702\times10^8}{RT_g}\right)$, $S_{CaCO_3} = 1.26\ m^2g^{-1}$
R_9	$R_9 = k_9\alpha_{s2}\rho_{s2}Y_{CaO}S_gY_{CO_2}a$	$k_9 = 490\exp\left(\frac{-1.75\times10^7}{RT_{s1}}\right)$, $a = \exp\left\lvert\frac{-571Y_{CaSO_4}}{(Y_{CaSO_4}+Y_{CaO}+Y_{CaSO_4})M_{CaCO_3}}\right\rvert$, $S_g = \begin{cases}-38.4T_{s2}+5.6\text{x}10^4 & T_{s2}\geq1252\ K\\ 35.9T_{s2}-3.67\text{x}10^4 & T_{s2}\leq1252\ K\end{cases}$

where d: solid particle diameter (m) k_i: reaction rate constant of reaction i, M_i: molecular weight of species i, p: gas pressure, p_i: pressure of species i, , D: diffusion coefficient, g: gravity acceleration, R_i: net production rate of reaction i, R: universal gas constant, Sh: Sherwood number, Sc: Schmidt number, ρ: density, Y_i: mass fraction of species i, ε: volume fraction, T: temperature and μ: viscosity

2.2 Simulation, Initial and Boundary Conditions

About the modeling setting, the employed viscous model was laminar. The density of gas species was calculated using an incompressible ideal gas law whiles the density of solid particle species was calculated using a volume-weighted-mixing-law. The specific heat capacities, thermal conductivities and viscosities for each phase were calculated using a mixing-law function of temperature, mass-weighted-mixing-law, and weighted-mixing-law, respectively. The maximum packing of solid particle was set as 0.60. The calculated time step was set as 0.001 s.

The other simulation, initial and boundary conditions for simulation are showed in Table 5 comparing with the experimental ones. For the initial condition, the industrial scale CFB boiler was filled with sand solid particles for using as the heating medium inside the system with static bed height of 0.61 m and volume fraction of 0.30. The temperature of each phase was set equal to 673 K. For the boundary condition, the velocities of gas phase in different inlet positions were already listed in Table 5. At the currently feeding location (fuel feed position), the velocities of fuel solid particle and $CaCO_3$ solid sorbent were set equally as 0.35 m/s with solid volume fraction of 8.81×10^{-4} and 2.30×10^{-4}, respectively. The inlet temperature at fuel feeding position was set as to 1,073 K due to the returning of unreacted fuel solid particle assumption. The inlet temperatures at primary, lower secondary air and upper secondary air positions were set as 673 K. There was no sand solid particle entered the system. At the outlet, the operating pressure was fixed as 101,325 Pa. The other important assumptions in this study were mono-sized solid particle and two-dimension model.

Table 5 Parameters used in the simulations

	Unit	Experiment	Simulation
Inlet gas velocity at primary air	m/s	1.40	1.40
Inlet gas velocity at lower secondary air	m/s	37.80	37.80
Inlet gas velocity at upper secondary air	m/s	48.41	48.41
Diameter of fuel solid particle	micron	700	700
Diameter of $CaCO_3$ solid particle	micron	350	350
Diameter of sand solid particle	micron	180	180
Density of fuel solid particle	kg/m^3	2,000	2,000
Density of $CaCO_3$ solid particle	kg/m^3	2,800	2,800
Density of sand solid particle	kg/m^3	2,659	2,659
Restitution coefficient	-	-	0.90
Specularity coefficient	-	-	0.01

3.0 RESULTS AND DISCUSSION

Before comparing the CFD results, the validation of the model and the time independency test (steady state time) were investigated. This study results showed that, after simulation time of 100 s, the absolute pressure began to stable indicating that the system starting to reach steady state time. After 100 s of simulation time, the chemical reactions were then analyzed and compared with the actual collecting experimental data from the power plant. Several modeling adjustments were performed to match the obtained simulation results with the real experimental information.

Table 6 illustrates the comparison of optimum simulation and obtained experimental results. It could be seen that, after the modeling adjustment, the simulation results were consistent with the experimental results. The outlet SO_2 concentration, O_2 concentration and system gas velocity were compared. The ranges of simulation results were similar to the ones of the experiment. This confirmed the correctness of the developed model. Then, this model was used in the following simulations. Figure 2 shows the corresponding contours of (a) O_2 and (b) SO_2 mole fractions for the optimum simulation. Both the gas concentrations were highest at the solid feeding location and then decreased throughout the industrial scale CFB Boiler due to the occurrence of chemical reaction.

Table 6 Comparison of optimum simulation and obtained experimental results

Case	O_2 (%)	SO_2 (ppm)	Velocity outlet (m/s)
Experiment	7	211 – 566	4.14 – 5.23
Simulation	7.22 – 10.85	319.70 – 432.17	3.46 – 4.18

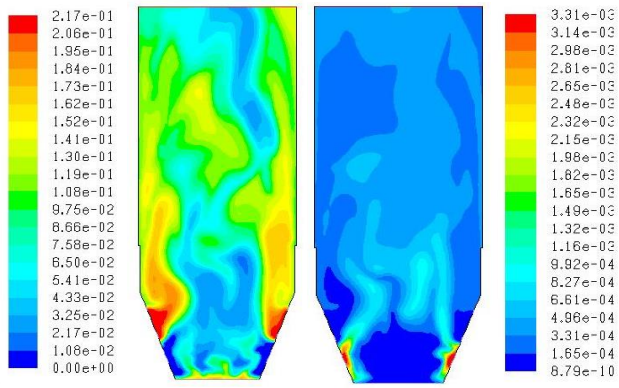

Figure 2 Contours of (a) O_2 and (b) SO_2 mole fractions for the optimum simulation (using 350 micron solid sorbent particle size and feeding solid sorbent at fuel feed position)

3.1 Effect of Solid Sorbent Feeding Position

In this study, the effect of solid sorbent feeding position on the SO_2 capture was investigated. The assumption is that the $CaCO_3$ solid sorbent should be fed at the position which has suitable temperature for desulfurization to occur. Here, three solid sorbent feeding position were compared which were the conventional solid sorbent feeding position at the fuel feed position and the other two new solid sorbent feeding position at the lower secondary air and upper secondary air positions. For comparison of the results, these three simulations were carried out with the same input amount of $CaCO_3$ solid sorbent.

Figure 3 shows the change in outlet CO_2 concentration, outlet O_2 concentration and outlet SO_2 concentration with three different solid sorbent feeding positions. From the results, the outlet O_2 concentrations were quite similar with three different solid sorbent feeding positions. The solid sorbent chemical reaction did not change the overall main combustion chemical reaction. However, slightly lower outlet O_2 concentrations were found from fuel feed, lower secondary air and upper secondary air positions, respectively. Therefore, the outlet CO_2 product concentrations were increased according to the following order: fuel feed, lower secondary air and upper secondary air positions. The outlet SO_2 concentrations for upper secondary air were lower than the outlet SO_2 concentration for lower secondary air and fuel feed positions, respectively. This is because the suitable higher system temperature with the upper secondary air position which accelerates the reaction rate of desulfurization chemical reaction.

In this study, the outlet SO_2 concentration for upper secondary air, lower secondary air and fuel feed positions were 384.39, 387.12 and 389.50 ppm, respectively. The difference of SO_2 gas with the changing of the location of solid sorbent injection was within 10 ppm, the location of solid sorbent injection therefore had a minor impact on improvement SO_2 capture efficiency. As stated above, this is because the slightly deviation in temperature between the feeding positions.

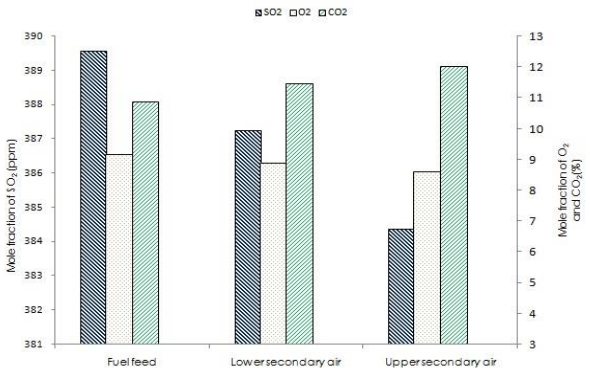

Figure 3 The outlet gas composition with three different solid sorbent feeding positions

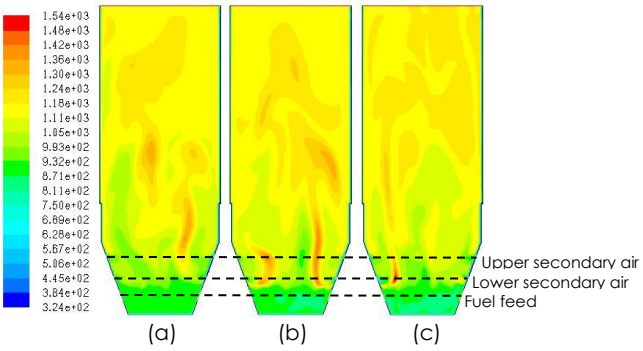

Figure 4 Contours of gas temperature (K) inside the riser section of industrial scale CFB boiler for (a) fuel, (b) lower secondary air and (c) upper secondary air feeding positions

Figure 4 shows the contour of gas temperature in industrial scale CFB boiler. All the solid sorbent feeding position exhibited quite similar gas temperature profiles. The results validated the above explanations that the suitable temperature inside the system was the reason for higher SO_2 capture [5]. This phenomenon occurred due to the buoyancy of high temperature gas product.

3.2 Effect of Solid Sorbent Particle Size

The effect of solid sorbent particle size on the SO_2 capture was also investigated. The assumption is that the $CaCO_3$ solid sorbent which has higher resident time will be appropriate to use inside this industrial scale CFB boiler. Here, three solid sorbent particle size were compared which were 200, 350 (conventional) and 500 micron. The other operating condition was similarly set for each case.

Figure 5 shows the change in outlet CO_2 concentration, outlet O_2 concentration and outlet SO_2 concentration with three different solid sorbent particles size. From the results, the increasing solid sorbent particles size decreased O_2 and SO_2 concentrations and increased CO_2 concentration. The solid sorbent particle with largest particle size will have higher system residence time which then appropriates to occur sorption reaction inside this industrial scale CFB boiler. Also, the large solid sorbent helps the mixing behavior inside the system which then assists the chemical reaction to occur.

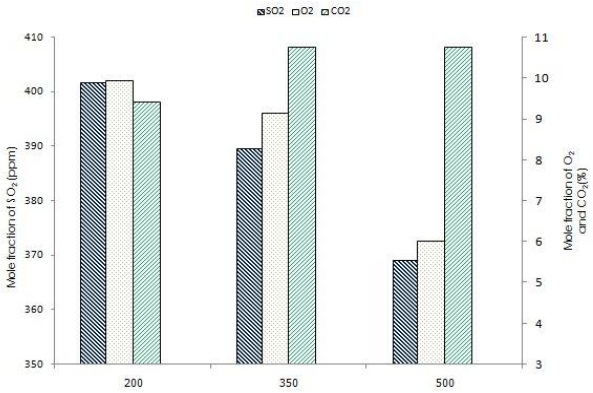

Figure 5 The outlet gas composition with three different solid sorbent particle sizes

In this study, the outlet SO_2 concentration for 200, 350 and 500 micron solid sorbent particle size were 401.76, 392.641 and 369.19 ppm, respectively. Figures 2 and 6 confirmed that the SO_2 mole fraction was lowest for 500 micron solid sorbent particle size.

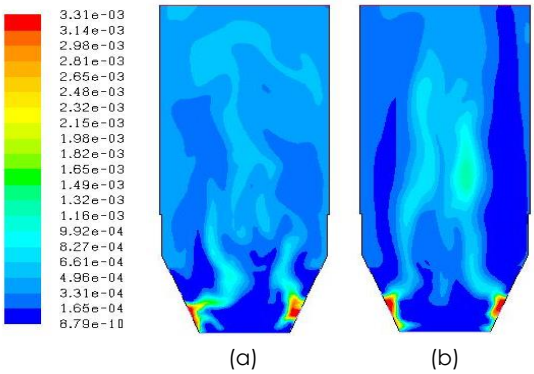

Figure 6 Contours of SO_2 mole fractions for solid sorbent particle size of (a) 200 and (b) 500 micron

4.0 CONCLUSION

In this study, the SO_2 capture modeling using $CaCO_3$ in industrial scale CFB boiler was developed using CFD simulation. The obtained CFD results were consistent with the real operation data.

For the effect of solid sorbent feeding position on SO_2 capture, entering solid sorbent at the upper secondary air position gave lower sulfur dioxide concentration than the one at the lower secondary air position and fuel feed position, respectively. This can be explained by the influence of suitable temperature at the upper secondary air position for desulfurization chemical reaction.

For the effect of solid sorbent particle size on SO_2 capture, the SO_2 capture was lowest when using the largest solid sorbent particle size due to the system hydrodynamics. The $CaCO_3$ solid sorbent which has higher residence time will be appropriate to use inside this industrial scale CFB boiler.

Acknowledgement

The PETROMAT, the Ratchadaphiseksomphot Endowment Fund 2015 of Chulalongkorn University (CU-58-059-CC), the Thailand Research Fund (TRG5780205), and the D.A. Research Center Co. Ltd are gratefully acknowledged.

References

[1] Staudt, J. E. 2011. Control Technologies To Reduce Conventional And Hazardous Air Pollutants From Coal-Fired Power Plants. M.J. Bradley & Associates LLC. United states of America

[2] Ryu, H., Grace, J. and Lim, C. 2006. Simultaneous CO_2/SO_2 Capture Characteristics of Three Limestones in a Fluidized-Bed Reactor. *Energy Fuels*. 1621-1628.

[3] Ma, L., Cao, L. and He, R. 2015. Numerical Study Of Pore Structure Effect On SO_2–CaO Reactions. *Chinese Journal of Chemical Engineering*. 23: 652-658.

[4] Arias, B., Cordero, J. M., Alonso, M., Diego, M. E. and Abanades, J. C. 2013. Investigation Of SO_2 Capture In A Circulating Fluidized Bed Carbonator Of A Ca Looping Cycle. *Industrial & Engineering Chemistry Research*. 52(7): 2700-2706.

[5] Shuai, W., Juhui, C., Guodong, L., Huilin, L., Feixiang, Z. and Yanan, Z. 2014. Predictions Of Coal Combustion And Desulfurization In A CFB Riser Reactor By Kinetic Theory Of Granular Mixture With Unequal Granular Temperature. *Fuel Processing Technology*. 126: 163-172.

[6] Chinsuwan, A., Dutta, A. and Janlasad, N. 2014. Prediction Of The Heat Flux Profile On The Furnace Wall Of Circulating Fluidized Bed Boilers. *Journal of the Energy Institute*. 87: 314-320.

[7] Qiu, G., Ye, J. and Wang, H. 2015. Investigation Of Gas–Solids Flow Characteristics In A Circulating Fluidized Bed With Annular Combustion Chamber By Pressure Measurement Sand CPFD Simulation. *Chemical Engineering Science*. 134: 433-447.

[8] Patankar, S. V. 1980. *Numerical Heat Transfer And Fluid Flow*. Hemisphere Publishing Corporation. New York

[9] Verstreeg, H. K. and Malalasekera, W. 2007. *An Introduction to Computational Fluid Dynamics: The Finite Volume Method*. 2nd ed. Longman Group Limited. England.

[10] Balakin, B. V., Hoffmann, A. C., Kosinski, P., and Rhyne, L. D. 2010. Eulerrian - Eulerian CFD Model For The Sedimentation Of Spherical Particles In Suspension With High Particle Concentrations. *Engineering Applications of Computational Fluid Mechanics*. 4(1): 116-126.

[11] Halwachs, M., Hofbauer, H. and Kampichler, G. 2009. Low Temperature Pyrolysis Of Agricultural Residues-First Results Of A Pilot Plant. *International Conference on Polygeneration Strategies.*

[12] Shuai, W., Juhui, C., Guodong, L., Huilin, L., Feixiang, Z. and Yanan, Z. 2014. Predictions Of Coal Combustion And Desulfurization In A CFB Riser Reactor By Kinetic Theory Of Granular Mixture With Unequal Granular Temperature. *Fuel Processing Technology*. 126: 163-172.

[13] Busciglio, A., Vella, G., Micale, G. and Rizzuti, L. 2009. Analysis Of The Bubbling Behaviour Of 2D Gas Solid Fluidized Beds Part II. Comparison Between Experiments And Numerical Simulations Via Digital Image Analysis Technique. *Chemical Engineering Journal*. 148: 145-163.

[14] Gungor, A. and Eskin, N. 2008. Two-Dimensional Coal Combustion Modeling Of CFB. *International Journal of Thermal Sciences*. 47: 157-174.

[15] Gungor, A. 2008. Two-Dimensional Biomass Combustion Modeling Of CFB. Fuel. 87: 1453-1468.

[16] Zhou, W., Zhao, C., Duan, L., Liu, D. and Chen, X. 2011. CFD Modeling Of Oxy-Coal Combustion In Circulating Fluidized

Bed. *International Journal of Greenhouse Gas Control.* 5(6): 1489-1497.
[17] Ross, I. B. and Davidson, J. F. 1982. The Combustion Of Carbon Particles In A Fluidized Bed. *Transactions of the institution of Chemical Engineers.* 60: 109-114.
[18] Rajan, R. R. and Wen, C. Y. 1980.A Comprehensive Model For Fluidized Bed Coal Combustors. *AIChE Journal.* 26: 642-655.
[19] Mattisson, T. and Lyngfelt, A. 1998. A Sulphur Capture Model For Circulating Fluidized-Bed Boilers. *Chemical Engineering Science.* 53: 1163-1173.
[20] Borgwardt, R. H. 1970. Kinetics Of Reaction Of SO_2 With Calcined Limestone. *Environmental Science & Technology*. 4: 59-63.
[21] Mattisson, T. and Lyngfelt, A. 1998. A Sulfur Capture Model For Circulating Fluidized-Bed Boilers. *Chemical Engineering Science*. 53: 1163-1173.
[22] Field, M. A., Gill, D. M., Morgan, B. B. and Hawskley, P. G. W. 1987. *Combustion of Pulverized Coal*. BCURA. Leatherhead. England.